

<https://doi.org/10.1038/s41538-024-00301-x>

Effect of freeze-thaw and PEF pretreatments on the kinetics and microstructure of convective and ultrasound-assisted drying of orange peel

Check for updates

Beatriz Llavata¹, Ronaldo E. Mello², Amparo Quiles³, Jefferson L. G. Correa² & Juan A. Cárcel¹ ✉

The main waste generated by juice industry comprises orange peels, which have a great upcycling potential once stabilized. Drying is the most used method for this purpose, but the high energy consumption prompts interest in its intensification. This study assessed the influence of freeze-thaw and pulsed electric field (PEF) pretreatments in conventional and airborne ultrasound-assisted drying (50 °C) of orange peels. None of these pretreatments alone got to reduce processing times significantly, but combined with ultrasound-assisted drying produced a significant shortening of the process. This was particularly important in the lower intensity PEF pretreatment tested (0.33 kJ/kg), indicating the existence of optimum conditions to carry out the pretreatments. Microstructure analysis revealed that the application of ultrasound during drying led to better preservation of the sample structure. Thus, the integration of pretreatment techniques to ultrasound-assisted drying may not only shorten the process but also help to preserve the original structure.

Oranges are one of the most widely cultivated fruit crops in the world¹. Much of the production goes to the juice industry, generating a large amount of waste, mainly made of peels². This by-product is an interesting source of biocompounds, such as fibers, vitamins or polyphenols³, so it has great value-adding potential to be added as an ingredient in the formulation of new products⁴. However, its high moisture content makes it susceptible to microbial or enzymatic deterioration reactions, which can reduce or even eliminate the bioactivity of these compounds. In this sense, hot air drying has been widely used because of its simplicity. This technique has significant advantages, such as prolonging product shelf life, reducing packaging costs, and decreasing storage and transport needs. However, this method does have significant drawbacks, such as high energy consumption⁵, which induces undesirable changes in the structure and the degradation of bioactive compounds present in the food, all of which are related to the long exposure of the product to high temperatures⁶. The application of treatments before drying is one of the strategies used to minimize these drawbacks and a wide variety of pretreatments can be found in the literature, from conventional techniques, such as osmotic pretreatments⁷, blanching⁸ or the freeze-thaw process⁹, to the use of new technologies, such as cold

plasma¹⁰, ultrasound application in liquid medium¹¹, electro-infrared treatments¹² or pulsed electric field application¹³. Most of these pretreatments aim to modify the food structure to make the moisture transport during the subsequent drying easier. Thus, in the case of freeze-thaw pretreatments, the formation of ice crystals during freezing may induce cell wall damage that can promote mass transfer during drying¹⁴. The velocity of the freezing process affects the number and size of the crystals. Thus, in a slow freezing process, few and large crystals are generated, which can break cellular walls and other structures. On the contrary, a fast freezing process produces numerous smaller crystals, which induce less cell damage¹⁵. In the case of pulsed electric field (PEF) technology, the application of high voltage electric pulses for a short time can induce pore formation in the cell membrane¹⁶. This effect is known as electroporation and can contribute to the increase in mass transfer rates during the dehydration process^{17,18}. The degree of electroporation achieved during the PEF pretreatment and its effects depend on the intensity of the treatment¹⁹.

Another completely different strategy to intensify convective drying consists of enhancing the drying process itself. In this sense, airborne power ultrasound (US) applied during the process can promote significant

¹Research Group of Analysis and Simulation of Agro-Food Processes (ASPA), Food Engineering Research Institute—FoodUPV, Universitat Politècnica de València, Valencia, Spain. ²Food Science Department, Universidade Federal de Lavras, Lavras, Minas Gerais, Brazil. ³Research Group of Food Microstructure and Chemistry (MIQUALI), Instituto Universitario de Ingeniería de Alimentos—FoodUPV, Universitat Politècnica de València, Valencia, Spain.

✉ e-mail: jcarcel@tal.upv.es

reductions in drying time^{20,21} due to the mechanical stress induced in the food tissues and the micro stirring generated at the solid-gas interfaces, improving moisture transport²². The extension of US effects is highly related to the internal structure of products²³. Therefore, the application of pretreatments that modify this structure can enhance the effect induced by the later application of ultrasound. Several studies have explored the combination of pretreatments with airborne ultrasound-assisted drying. For instance, Zhu et al.²⁴ assessed the influence of blanching and brining of apple, Corrêa et al.²⁵ studied the application of solid-liquid pretreatments of pineapple, and Rojas et al.²⁶ tested ethanol pretreatment of apple chips; all of these pretreatments applied before the ultrasound-assisted drying. Other authors have also examined the combination of several pretreatments before a conventional drying process. Thus, Liu et al.²⁷ evaluated the combination of freeze-thaw and ultrasound pretreatment in a liquid medium before drying, and Xu et al.²⁸ studied the effect of freeze-ultrasound thawing and freeze-air ultrasound thawing pretreatments on the vacuum freeze-drying of okra. To the authors' knowledge, however, there are no studies that assess the influence of freeze-thaw pretreatment on ultrasonic-assisted drying. As regards the combination of PEF pretreatment and US-assisted drying, the only previous analyses that have been found are those carried out by the authors regarding the antioxidant properties of orange peels²⁹ and kiwifruits³⁰.

Therefore, the aim of this study was to evaluate the effect of two different pretreatments, freeze-thaw and pulsed electric field (PEF), at two different levels on the kinetics of conventional and ultrasound-assisted drying of orange peels. Moreover, the impact of these pretreatments and the two types of drying on the final structure of the dried product was also assessed.

Results

Drying experiments

The initial moisture content of orange peel was 2.9 ± 0.2 kg water/kg d.m. During the conventional drying of samples, it was observed that the freeze-thaw pretreatment affected the process kinetics. The drying kinetics of slowly frozen samples (SF-AIR) were slightly faster than those of non-pretreated ones (UP-AIR). However, the kinetics of fast frozen samples (FF-AIR) were significantly slower. Among the samples treated with pulsed electric field (PEF), only those pretreated at low intensity (LiPEF-AIR) had slightly shorter, but significant, drying times than the UP-AIR sample (Table 1).

The application of power ultrasound (US) during drying significantly shortened the process, regardless of the pretreatment considered (Fig. 1). Thus, the drying time required for UP-AIR samples to reach a moisture

content of 0.55 ± 0.02 kg w/kg d.m. was reduced by 27.2% when US was applied during drying (UP-US) (Table 1). Overall, the combination of pretreatments and ultrasound-assisted drying accelerated the process. Specifically, the drying experiments of SF-US, LiPEF-US and HiPEF-US samples were significantly ($p < 0.05$) faster than the UP-US and, compared to UP-AIR samples, showed drying time reductions of 35.0%, 40.0%, and 35.6% respectively. On the contrary, the combination of fast freezing and ultrasound-assisted drying (FF-US) resulted in slower kinetics than the ultrasound-assisted drying of unpretreated samples (UP-US).

Modeling of drying kinetics

The modeling of experimental drying kinetics permitted the quantification of the differences among pretreatments (freeze-thaw and PEF pretreatments) and drying techniques (conventional and US-assisted) considered. The fit of the selected model to the experimental data was adequate, as shown by the percentage of explained variance (%Var), above 99.7% in every experiment (Table 1). Moreover, a good agreement was observed between experimental and calculated moisture contents (Fig. 2).

The results showed that, compared to the non-pretreated (UP-AIR) samples, the application of pretreatments before conventional drying of orange peel decreased the effective diffusivity identified (D_{eff}). These differences were significant ($p < 0.05$) in the case of freeze-thaw pretreated samples (Table 1). On the other hand, the identified mass transfer coefficient (k) was greater in the pretreated samples, being the differences with UP-AIR

Table 1 | Drying time (min), effective diffusivity (D_{eff}) (m^2/s), mass transfer coefficient (k) ($kg/m^2 \cdot s$) and the percentage of variance explained (%Var) of the different pretreatments and drying conditions studied

| Drying condition | Drying time (min) | $D_{eff} \cdot 10^{-10}$ (m^2/s) | $k \cdot 10^{-4}$ ($kg/m^2 \cdot s$) | %Var |
|------------------|------------------------|--------------------------------------|--|-------|
| UP-AIR | 300 (18) ^e | 6.6 (0.7) ^{cd} | 8.5 (0.5) ^a | 99.85 |
| FF-AIR | 363 (10) ^f | 4.1 (0.1) ^a | 8.9 (0.5) ^a | 99.82 |
| SF-AIR | 297 (21) ^{de} | 5.4 (0.2) ^b | 11 (2) ^b | 99.94 |
| LiPEF-AIR | 281 (12) ^d | 5.8 (0.4) ^{bc} | 10.1 (0.8) ^{ab} | 99.78 |
| HiPEF-AIR | 287 (6) ^{de} | 5.3 (0.3) ^{abc} | 11.0 (0.1) ^b | 99.85 |
| UP-US | 218 (3) ^b | 8 (1) ^{de} | 15 (3) ^f | 99.70 |
| FF-US | 245 (6) ^c | 6.4 (0.3) ^{bcd} | 11.9 (0.5) ^b | 99.80 |
| SF-US | 195 (13) ^a | 8.3 (0.8) ^a | 17 (2) ^d | 99.95 |
| LiPEF-US | 180 (8) ^a | 11 (2) ^f | 14.6 (0.6) ^c | 99.80 |
| HiPEF-US | 193 (6) ^a | 8.0 (0.6) ^a | 15.1 (0.8) ^c | 99.71 |

Values are reported as the average (standard deviation). Different letters in the same column indicate significant differences according to an LSD test ($p < 0.05$).

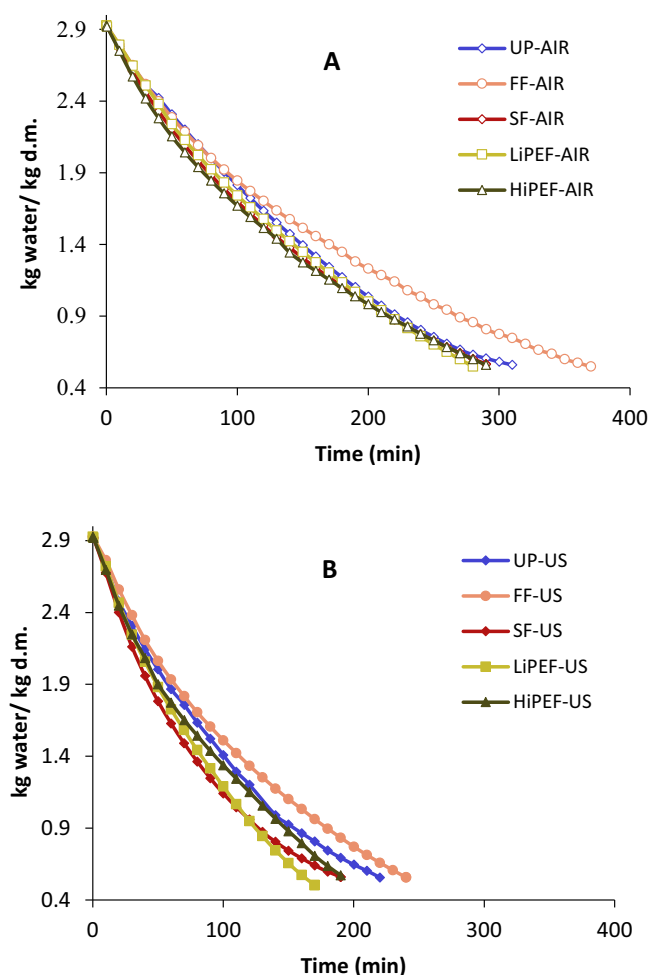


Fig. 1 | Experimental drying kinetics (50 °C) of orange peel obtained for conventional drying (AIR, Fig. 1A) and ultrasound-assisted convective drying (US, Fig. 1B). Un-pretreated (UP), freeze-thaw pretreated with slow (SF) and fast (FF) freezing, and PEF pretreated samples (1.25 kV/cm) at low (8 pulses, LiPEF) and high (24 pulses, HiPEF) intensity.

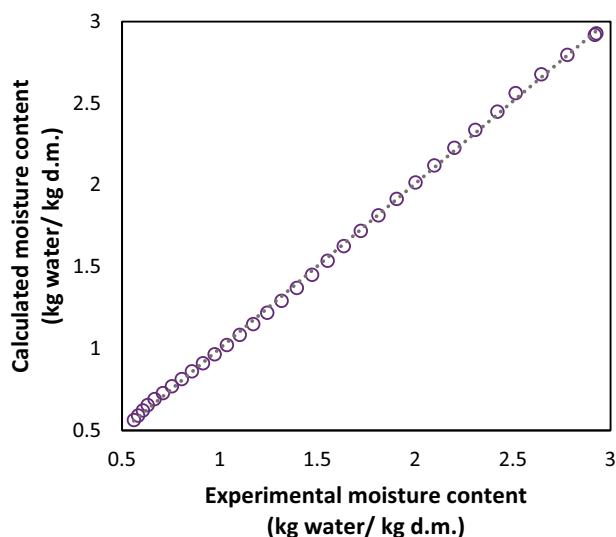


Fig. 2 | Goodness of model fit. Experimental versus calculated moisture content (kg water/ kg d.m.) of the orange peel during conventional (UP-AIR) drying at 50 °C.

significant ($p < 0.05$) in the case of SF-AIR and LiPEF-AIR samples (Table 1).

The application of airborne ultrasound during drying significantly ($p < 0.05$) increased both D_{eff} and k (Table 1), being both parameters 21 and 76% greater in UP-US than in UP-AIR samples. As for the freeze-thaw pretreatments, the velocity of freezing had a significant impact on both kinetic parameters. In fact, the FF-US samples presented D_{eff} and k values that were not only significantly ($p < 0.05$) lower than those of the SF-US samples, but even lower than UP-US. As for PEF pretreatments, no significant differences were observed among the D_{eff} and k values identified for HiPEF-US and UP-US samples. However, the LiPEF-US experiments showed the significant ($p < 0.05$) greatest values of both modeling parameters (Table 1) among all the conditions tested.

Effects of drying on the microstructure

Orange peel consists of two types of parenchyma cell tissues, albedo and flavedo. The outer layer, flavedo, is made up of small, elongated cells with almost no intercellular spaces. The albedo, the white inner layer, has rounded cells with large intercellular spaces. Conventional drying produced a significant structural modification of the orange peel tissues, as shown in the light microscope images included in Fig. 3. In the UP-AIR samples, most of the cells appeared disintegrated, broken, and separated from each other by large intercellular spaces, so it was not possible to differentiate flavedo or albedo tissues with certainty. The parenchyma was mainly formed by the apoplast or the space outside the plasmalemma.

The freeze-thaw and PEF pretreatments induced changes in the structure of conventionally dried samples. Thus, the microscope images of frozen-thawed samples (Fig. 3) showed a degraded structure with large intercellular spaces. However, the cell walls appeared better defined than in the case of UP-AIR samples. This definition was more marked in the cells of FF-AIR samples than in those of the SF-AIR samples. The PEF pretreated samples also presented an unstructured parenchyma consisting of deformed or partially disintegrated cells and large intercellular spaces. The samples pretreated with PEF presented highly blurred cell walls compared to the UP-AIR samples. This fact was more intense in HiPEF-AIR than in LiPEF-AIR. Thus, the image presented a deeper blue coloration, indicating a greater dispersion of the cell wall compounds (cellulose fibrils, cellular cement...).

The application of US during drying significantly contributed to preserving the original structure of fresh samples. As can be observed in the microstructure images of Fig. 4, the two main tissues (flavedo and albedo) of

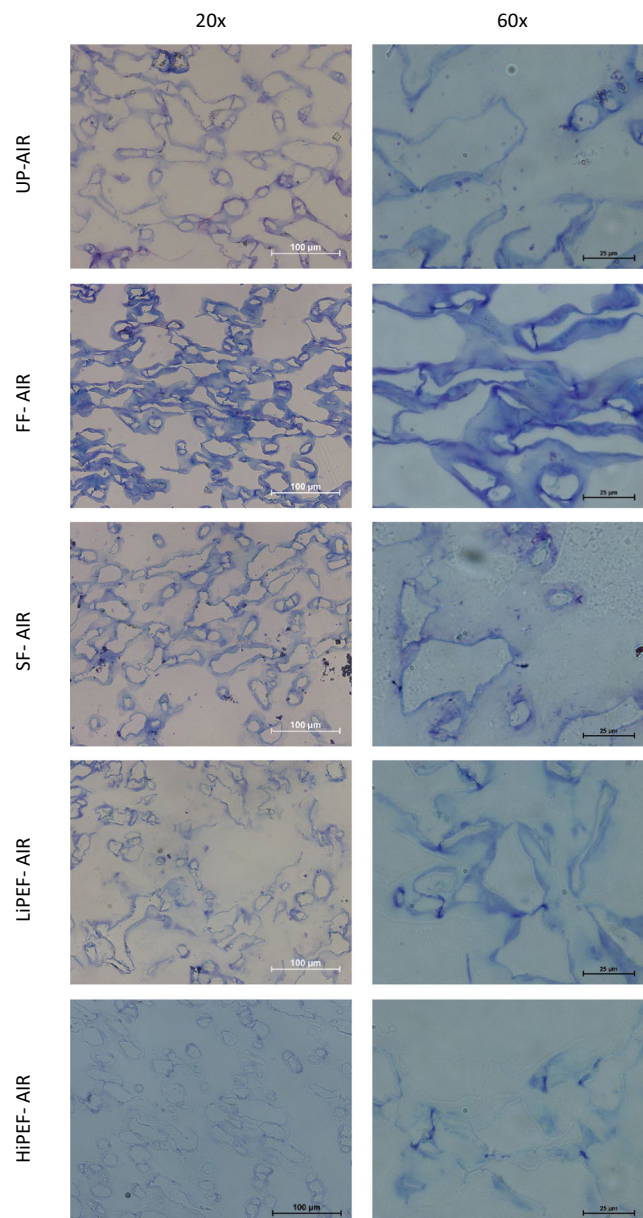


Fig. 3 | Microstructure of conventionally dried orange peel. Light microscope images of parenchymatic cells of orange peels conventionally dried (AIR) at 50 °C: un-pretreated (UP), freeze-thaw pretreated with slow (SF) and fast (FF) freezing, and PEF pretreated samples (1.25 kV/cm) at low (8 pulses, LiPEF) and high (24 pulses, HiPEF) intensity.

orange peel were clearly distinguishable in all cases, regardless of the pretreatment considered, and in contrast of the conventionally dried samples (Fig. 3). Thus, UP-US samples showed almost intact cells after drying. The cellular walls were closely packed with no discontinuities and, consequently, dense in appearance. It was also possible to observe the plasmalemma remained close to the cellular wall. The frozen-thawed or PEF pretreated samples presented a slightly more disordered structure with swollen cell walls. As in the case of freeze-thaw conventionally dried samples, the FF-US maintained a more complete structure than the SF-US, but with the walls highly warped. Moreover, the SF-US samples presented some breaks in the cell wall that were not observed in FF-US. Regarding PEF pretreated samples, the cell deformation and the blueish color of images of HiPEF-US samples indicated some tissue degradation. On the contrary, cells of LiPEF-US samples appeared better defined and compacted than in the HiPEF-US, which means better preservation of raw matter structure.

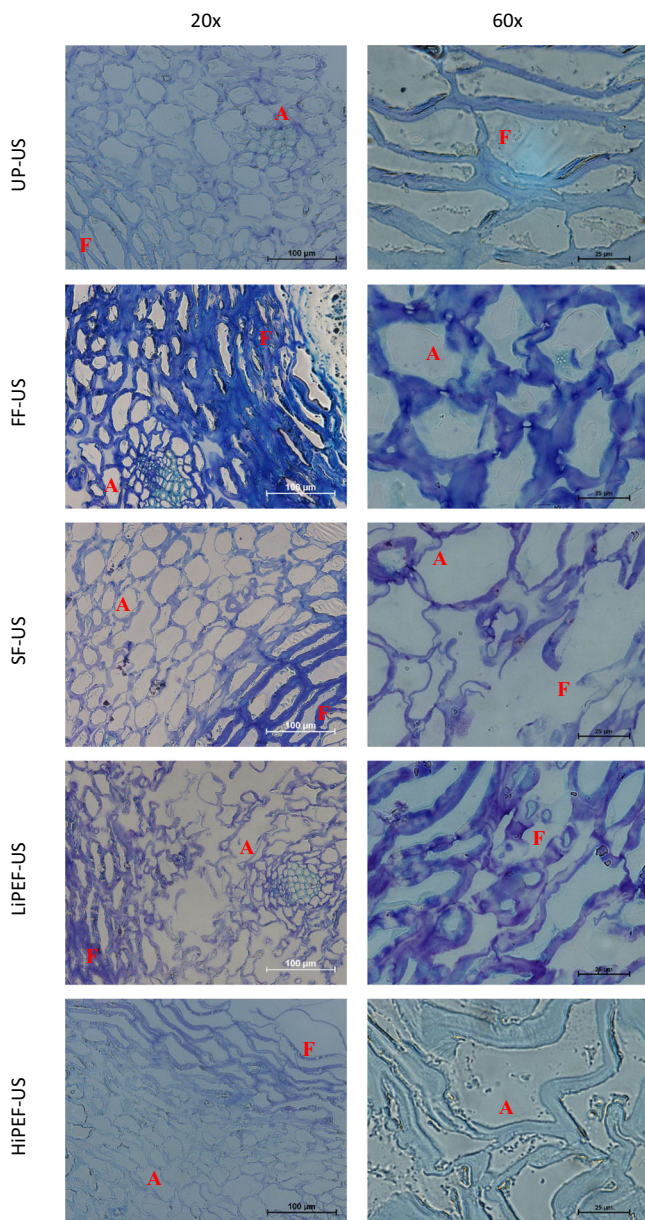


Fig. 4 | Microstructure of ultrasonically assisted dried orange peel. Light microscope images of parenchymatic cells (A, albedo; F flavedo) of orange peel ultrasonically assisted dried (US) at 50 °C: Un-pretreated (UP), freeze-thaw pretreated with slow (SF) and fast (FF) freezing, and PEF pretreated samples (1.25 kV/cm) at low (8 pulses, LiPEF) and high (24 pulses, HiPEF) intensity.

Discussion

The experimental results indicated a significant influence of freeze-thaw and pulsed electric field (PEF) pretreatments on both conventional and ultrasound-assisted drying kinetics and the final structure of orange peel. Thus, in the case of the freeze-thaw pretreatments, the effect of freezing velocity on drying kinetics could be attributed to the differences in the ice crystal formation process that took place under the two conditions tested, fast and slow freezing. Fast freezing resulted in the formation of many small ice crystals that were uniformly distributed inside the cell. On the contrary, when slow freezing occurred, the ice nucleation rate was slower than the ice growth, generating large ice crystals spread throughout the extracellular region³¹. These different ice crystal characteristics and distributions can generate different structural changes that could promote dissimilar effects on the mass transport process. The small ice crystal generated in the fast freezing (FF) did not break the cell membranes, but swollen the cell walls

and dispersed some of the wall components. This important disorder induced made the water release difficult. This made the moisture diffusion inside samples difficult and would explain the delay of FF-AIR drying compared with UP-AIR. On the contrary, the larger ice crystals generated during slow freezing (SF) could break cell walls, making easier moisture transport, which would explain the slight increase in the drying rate of SF-AIR samples. In this sense, some studies have found enhancement of the drying process through applying freeze-thaw pretreatments. For instance, Vallespir et al.¹⁵ reported that freeze-thaw pretreatments at different freezing temperatures (−20, −80, and −196 °C) induced drying time reductions in beetroots (11–16% shorter compared to control samples), apples (25%) and eggplants (12–32%). Similarly, Santos et al.³² also found that freeze-thaw pretreatment of papaya shortened drying (32%), while Guo et al.³³ observed significant reductions of drying process (20–50%) in the case of garlic. However, other authors reported no drying time reduction induced by frozen-thaw pretreatments, such as Chen et al.³⁴ in the case of blueberries.

Regarding PEF pretreatments, the shortening of the drying process observed (Table 1) could be attributed to the permeabilization of the cell membrane, which could lead to an increase in the moisture diffusivity³⁵. Nevertheless, the drying time difference between PEF pretreated and UP-AIR samples was small. PEF can also soften the food matrix, resulting in a collapse of the cell structure, which compromises the diffusive process³⁶. Therefore, it is important to note that the effect of the PEF pretreatment on drying kinetics is very complex. It depends not only on the electrical conditions applied but also on the product considered, the drying temperature, or the drying method. Thus, Arevalo et al.³⁷ found that the same PEF pretreatment that shortened the drying of potatoes did not have the same effect on apples. Alam et al.³⁸ stated that carrot drying was shortened by pretreating with PEF at 50 and 60 °C, but not at 70 °C, while parsnip drying was shortened at 60 and 70 °C, but not at 50 °C. Likewise, Pérez-Won et al.³⁹ reported an acceleration in the freeze-drying and vacuum microwave drying rate of some products pretreated with PEF but a slowing down in the case of convective drying. On the contrary, Wiktor et al.⁴⁰ observed that although the PEF pretreatment shortened the convective drying process, it did not influence microwave-assisted air drying.

The ultrasound-assisted drying significantly reduced the process time of the conventional drying (Table 1), which is consistent with previous studies of different citrus by-products like lemon peel⁴¹ and orange peel⁴². This fact was probably related to the mechanical effects generated in the food matrix that accelerated the mass and heat transfer processes⁴³. The structural changes induced by pretreatments affected the magnitude of US effects, likely because they altered the impedance of samples. Thus, these structural changes can modify the elastic properties of samples. The relationship between the elastic properties and the ultrasonic velocity is widely known, which in turn affects the acoustic impedance²³ and then the air-sample impedance mismatch. In this sense, the products with low acoustic impedance get a better coupling with the drying air. This facilitates the US propagation and makes its effects more noticeable, enhancing the mass transfer²². Therefore, while the influence of pretreatment applied alone was modest, they could create a suitable matrix in the products that enhanced the effects of airborne ultrasound when applied during drying.

The modeling of drying kinetics provided a better understanding of the mechanisms of the observed effects. About the internal transport of conventionally dried samples, the significantly lower values of effective diffusivity (D_{eff}) identified in pretreated samples can be attributed to the disorders in the cell matrix induced by the pretreatments. These D_{eff} values were significantly different ($p < 0.05$) in the case of freeze-thaw pretreatments, which indicates that the effects on the cell matrix of the ice crystals generated during sample freezing were greater than those induced by PEF pretreatments. However, other authors have reported higher diffusivity values when freezing pretreatments were applied^{44,45} to products such as carrot or apple. This could be attributed to the different initial structure of the materials studied and, therefore, the different effects induced in the matrix. Regarding the external transport, a significantly greater mass

transfer coefficient (k) was observed in SF-AIR and HiPEF-AIR. This increase might be linked to some damage caused by the pretreatments to the outer waxy layer of the flavedo, which reduced the natural resistance of the orange peel to dehydration. In the case of freeze-thaw pretreatment, the freezing step could modify the product surface and increase the area in contact with the air. This could reduce external resistance and cause greater moisture transfer⁴⁶. In the case of PEF pretreatment, it could generate greater water release to the surface, producing a moisture-saturated surface, which increased the influence of the external resistance on the drying process as compared to the internal one. A similar effect has been previously reported for the drying of spinach⁴⁷ and onion³⁶.

The US application during drying led to higher D_{eff} figures, whichever the pretreatment considered. The ultrasonic waves could generate successive contractions and expansions of the matrix (sponge effect) and produce internal microcracks that reduced the internal resistance to mass transfer. Likewise, the increase in k indicated a lower external resistance, likely linked with the pressure and velocity variations at the surface level produced by US vibration⁴⁸, which reduced the diffusion boundary layer and enhanced the external moisture transport. However, the magnitude of these effects depended on the pretreatment considered. In the case of freeze-thaw pretreatments, the freezing velocity affected D_{eff} and k . This fact can be related to structural changes induced by freezing, which developed a more prone structure to the US effects in SF-US pretreated samples (higher values of both D_{eff} and k), likely linked to the partial break of cell membranes. In contrast, FF-US showed a less susceptible structure, probably related to the swelling of the cell walls (Table 1). No studies have been found about the combined application of freeze-thaw pretreatments and ultrasonically assisted drying. As for PEF pretreatments, it was also observed that LiPEF-US resulted in higher values of both kinetics parameters, D_{eff} and k . In this case, a moderate electroporation could reduce the impedance of the matrix, making easier the propagation of US energy²³. On the contrary, the greater PEF intensity of the HiPEF-US pretreatments could have induced a significant collapse in the structure, making ultrasound propagation difficult. This last fact has been previously reported by Wiktor et al.⁴⁹ in carrot drying. The results would indicate the existence of an optimum PEF pretreatment, which produces adequate internal effects that favor US assistance when applied during drying. The similar D_{eff} values identified in the SF-US and HiPEF-US experiments could point out that both treatments induced a similar effect in the internal structure of the samples.

In summary, compared with control samples (UP-AIR), the lower values of D_{eff} identified in the drying experiments carried out with pretreatments indicated an increase in the internal resistance to mass transfer. This increase could be attributed to the structural disorders induced, which in the case of SF-AIR, LiPEF-AIR, and HiPEF-AIR can be related to a partial destruction of the cell structure, while in FF-AIR with a cell wall swollen effect. At the sample surface level, these effects could damage the outer waxy layer, reducing the external resistance to mass transfer, as shown the greater value of k obtained, except for FF-AIR samples. The swollen cell wall effect could counteract the waxy layer degradation in this case.

Ultrasound application during drying significantly reduced both internal and external mass transfer resistance. However, the structural changes induced by the tested pretreatments affected the intensity of ultrasound effects. Thus, the swollen effect of FF-US pretreatment on the cell walls could attenuate ultrasonic vibration, decreasing ultrasound influence on internal and external mass transfer resistance. In the case of SF-US, the internal disorders did not significantly affect the internal influence of ultrasound but significantly weakened the external one, probably linked with the development of a more porous surface that was more prone to the ultrasound effects. Regarding PEF treatments, the structural changes induced at the adequate intensity (LiPEF-US) enhanced the internal ultrasound influence, but no significant influence of these changes was observed on the external resistance.

The analysis of the microstructure of orange peel dried samples contributed to understanding the effects induced by both pretreatments and drying process. Thus, the freeze-thaw pretreated samples presented a highly

altered structure, linked to both the ice crystals generated during freezing, which damaged the cell walls and produced the lysis of vacuoles²⁷, and the later drying. Specifically, the disorganized structure of FF-AIR, with areas with visible but blurred cell walls and areas without them (Fig. 3), could make moisture diffusion difficult⁵⁰, and it would explain that the drying process of these experiments was longer (Table 1) than control ones. On the contrary, the large ice crystals formed during slow freezing could make the diffusion of water through the cell walls easier. This caused a greater swelling of the cell walls, destroying the middle lamella, as shown by the slightly colored walls in Fig. 3. However, this structural modification was not enough to shorten the drying significantly compared to the UP-AIR samples. Other authors have also observed that the velocity of the freezing pretreatment can induce different changes in the microstructure of products such as raisin grapes⁵¹ or potatoes³¹ reporting obstruction of capillary ducts, formation of large cracks and deformations of cells in slowly frozen samples.

Regarding the PEF pretreated samples, it was observed that PEF damaged the structure, generating large pores, deformed membranes, and cell lysis⁵². These facts were more marked in the more intense PEF treatment tested (HiPEF-AIR), which could make the moisture movement inside the samples difficult and explain the lower values of effective diffusivity identified.

The airborne US application during the drying process helped to preserve the orange peel structure. The continuous contraction and expansion of orange peel samples could induce the warp of cells without breaking the structure, making the inner moisture transport easier. This shortened the drying process, avoiding lengthy exposure to high temperatures that could induce tissue damage. Moreover, the ultrasonic waves could release intercellular air and, therefore, reduce the pressure difference between the sample inside and the sample surface, mitigating sample contraction during drying. Puig et al.⁵³ also reported that drying assisted with ultrasound preserved the structure of eggplant better than conventional drying.

However, the structure of dried samples differed regarding the combination of the pretreatments and ultrasound-assisted drying. Thus, thick warped cell walls were observed in FF-US samples, which could make difficult the water transport through them and would explain why these samples presented the lowest D_{eff} and k identified among the ultrasound-assisted dried samples. On the contrary, the breaks found in the cell walls of SF-US samples, likely linked with the formation of large ice crystals during freezing, would help the inner moisture transport to the surface and from there to the surroundings as showed the greatest k value obtained and linked to the shorter drying time of these experiments compared to those of the UP-US sample. Chao et al.⁵⁴ stated that a freezing pretreatment could create microcracks and even irreversible structural damage to the cell walls, middle lamella and protoplasm. In this sense, it was difficult to distinguish the middle lamella and protoplast in the SF-US images (Fig. 4). In the case of the PEF pretreated samples, it was observed some differences between HiPEF-US and LiPEF-US experiments. Thus, LiPEF-US samples presented a less damaged structure than HiPEF-US ones, which could improve the ultrasonic energy transmission and could explain the highest D_{eff} values obtained.

Therefore, the application of ultrasound during drying not only contributed to the shortening of the drying process but also had a preserving effect on the microstructural tissue. When applied in adequate conditions, the structural changes induced by the freeze-thaw or PEF pretreatments can significantly intensify the US effects of orange peel, a slow freezing process in the case of freeze-thaw pretreatments and a moderate intensity for PEF pretreatment. Particularly, this last combination, the LiPEF-US, provided the fastest procedure, preserving the initial structure of orange peel.

Methods

Raw material

Valencia Late var. orange (*Citrus sinensis*) samples, acquired at a local market in Valencia (Spain), were stored at 4 °C until the drying experiments. The oranges were washed and peeled by hand with a sharp knife. Then,

Table 2 | Experiment codes in terms of the pretreatments and drying conditions considered

| Drying | Pretreatments | | | | |
|------------------------------|---------------|---------------|---------------|---------------|----------------|
| | Unpretreated | Freeze-thaw | | PEF | |
| | | Fast freezing | Slow freezing | Low intensity | High intensity |
| Conventional (AIR) | UP-AIR | FF-AIR | SF-AIR | LiPEF-AIR | HiPEF-AIR |
| Ultrasonically assisted (US) | UP-US | FF-US | SF-US | LiPEF-US | HiPEF-US |

orange peel slices of $5.0 \times 2.5 \times 0.3$ cm, containing only flavedo and albedo tissues, were obtained. The samples presented an initial moisture content of 2.9 ± 0.2 kg water/kg d.m., which was in the range reported in other studies^{55,56}.

Pretreatments

Freeze-thaw pretreatment. In these pretreatments, two freezing conditions were considered: fast and slow. For fast freezing (FF) processes, the samples were covered with a plastic film to avoid moisture loss and frozen in a blast chiller shock freezer (HIBER, model RDM051S, Italy) at -35.0 ± 0.3 °C for 2 h. For the slow freezing (SF) treatment, the samples, also packed in plastic film, were introduced in a domestic freezer (Liebherr SGN 3063, Switzerland) at -18.0 ± 0.7 °C for 24 h. In this case, air turbulence around samples was avoided to make difficult the convection heat transfer and delay as possible the freezing process. Before drying, both FF and SF samples were thawed at 25 ± 1 °C until the internal temperature was constant.

Pulsed Electric Field (PEF) pretreatment. The PEF pretreatments were performed with a PEF system (EPULSUS-PM1, Energy Pulse System, Lisbon, Portugal), which generated high-intensity monopolar pulses. The pretreatments were carried out with an electric field strength of 1.25 kV/cm, a frequency of 10 Hz and a pulse width of 25 μ s. The treatment chamber containing the samples was filled with tap water (electrical conductivity of 1.04 ± 0.03 mS/cm), used as the electricity conductor medium. Two different levels of treatment intensity were also tested in this case: one of lower intensity (LiPEF), applying eight pulses, and another of higher intensity (HiPEF), applying 24 pulses. These treatments meant an energy input of 0.33 and 0.98 kJ/kg, respectively.

In addition to these four pretreatments, unpretreated (UP) samples were also considered as control.

Drying experiments

The pretreated (FF, SF, LiPEF and HiPEF), as well as the control (UP) samples, were dried in an ultrasound-assisted convective dryer, previously described by Llavata et al.⁴³. For each run, 18 slices of orange peel samples were randomly placed in a sample holder ensuring homogeneous air distribution. The experiments were performed at 50 °C and 1 m/s, and the weight was automatically recorded every 10 min with a balance coupled to the dryer. The drying process was finished when the samples lost 60% of their initial weight.

Two types of drying experiments were carried out for each pretreatment: a conventional drying process (AIR) and an ultrasound-assisted convective drying process (US) (Table 2). The airborne power ultrasound was applied through the walls of the drying chamber, an aluminum-vibrating cylinder excited by a piezoelectric transducer, working at a resonance frequency of 21.8 ± 0.4 kHz, and supplied with a constant power of 50 W. All the experiments were performed at least in triplicate.

Modeling

Experimental data modeling was performed to quantify the influence of pretreatments and the effect of ultrasound application during drying on the process kinetics. For this purpose, it is more adequate the use of mechanistic models than empirical ones due to, even though these last can accurately describe the drying kinetics, they are only valid just for the conditions

considered to achieve the experimental data, they usually neglect the fundamentals of drying process and their parameters have no physical meaning. Therefore, in this study, a model based on the diffusion theory was chosen. Thus, from the combination of a mass microscopic balance and the Fick's law of diffusion and assuming that the samples followed an infinite slab behavior with unidirectional moisture flow, it was obtained the Eq. (1)

$$\frac{\partial W(x, t)}{\partial t} = D_{\text{eff}} \frac{\partial^2 W(x, t)}{\partial x^2} \quad (1)$$

where W is the moisture content (kg water/kg dry matter, d.m.), D_{eff} is the effective diffusivity (m^2/s), t is the time (s), and x is the direction of the water transport (m). To solve Eq. (1), sample moisture content was assumed to be uniform at the beginning of the drying process. Both internal and external resistance to moisture transport were considered in the model as a boundary condition Eq. (2).

$$-D_{\text{eff}} \cdot \rho_{\text{ss}} \frac{\partial W(L, t)}{\partial x} = k(a_w(L, t) - \varphi_{\text{air}}) \quad (2)$$

where ρ_{ss} is the density of dry solid (kg d.m./ m^3) reported by Garcia-Perez et al.⁵⁷, k is the mass transfer coefficient (kg water/ m^2s), a_w is the water activity, L is the thickness of the orange peel (0.005 m), and φ_{air} is the relative humidity of drying air. The equilibrium conditions were estimated from the moisture sorption isotherms reported by Kammoun Bejar⁵⁸.

Equation 2 is a continuity condition. Thus, the moisture transport from the inner part of the samples to the outer surface, which took place by diffusion (the left-hand side of Eq. 2), moved by convection from the sample surface into the drying air (the right-hand side of Eq. 2). The model was solved by applying a finite differences methodology. The Matlab 2015B® (The Mathworks, Inc, Natick, USA) software was used to identify the kinetic parameters, effective diffusivity (D_{eff}) and mass transfer coefficient (k). The SIMPLEX method available in Matlab 2015B® was applied to solve the optimization problem, which was to minimize the squared differences between the experimental and calculated moisture contents.

The percentage of variance explained (%Var) by the model was determined to verify how accurately the model fitted (Eq. 3).

$$\% \text{Var} = \left[1 - \frac{S_{\text{calc}}^2}{S_{\text{ex}}^2} \right] 100 \quad (3)$$

where S_{calc}^2 is the calculated variance and S_{ex}^2 is the experimental variance.

Microstructure

To study the combined effects of the pretreatments and the considered drying conditions on the final dried product's internal structure, the dried samples' microstructure was analyzed using light microscopy. The samples were cut into cubes (3 mm³) and then fixed with a 25 g/L glutaraldehyde solution (0.025 M phosphate buffer, pH 6.8, at 4 °C, 24 h). Afterward, they were post-fixed with a 20 g/L OsO₄ solution (1.5 h) and dehydrated using a graded ethanol series (300, 500, 700, 960, and 1000 g/kg). Finally, they were contrasted in 40 g/L uranyl acetate dissolved in ethanol and embedded in epoxy resin (Durcupan, Sigma-Aldrich, St. Louis, MO, USA). The samples were cut using a Reichert Jung ultramicrotome (Leica Microsystems, Wetzlar, Germany). Thin sections (1.0 μ m) were stained with 2 g/L

toluidine blue and examined in a Nikon Eclipse E800 light microscope (Nikon, Tokyo, Japan).

Data analysis

The significance of the results was assessed using a multifactorial ANOVA. A residuals analysis was carried out to identify anomalous experiments and to determine if they follow a normal distribution with a constant variance, conditions which ensure the validity of the ANOVA. The LSD (least significance difference) intervals ($p < 0.05$) were estimated using the software Statgraphics Centurion XVI (StatPoint Technologies, Inc) to differentiate the significantly different conditions.

Data availability

Data available under request to the corresponding author: Juan A. Carcel (jcarcel@tal.upv.es).

Received: 11 March 2024; Accepted: 12 August 2024;

Published online: 24 August 2024

References

1. Simons, T. et al. Chemical and sensory analysis of commercial Navel oranges in California. *npj Sci. Food* **3**, 1–11 (2019).
2. Wang, Z. et al. Extraction and recovery of bioactive soluble phenolic compounds from brocade orange (*Citrus sinensis*) peels: effect of different extraction methods thereon. *Lwt* **173**, 114337 (2023).
3. Xue, P. et al. Release characteristic and mechanism of bound polyphenols from insoluble dietary fiber of navel orange peel via mixed solid-state fermentation with *Trichoderma reesei* and *Aspergillus niger*. *LWT* **161**, 113387 (2022).
4. Wang, Y. & Jian, C. Sustainable plant-based ingredients as wheat flour substitutes in bread making. *npj Sci. Food* **6**, 1–16 (2022).
5. Llavata, B., Picinelli, A., Simal, S. & Cárcel, J. A. Cider apple pomace as a source of nutrients: evaluation of the polyphenolic profile, antioxidant and fiber properties after drying process at different temperatures. *Food Chem. X* **15**, 100403 (2022).
6. Borsini, A. A., Llavata, B., Umaña, M. & Cárcel, J. A. Artichoke by products as a source of antioxidant and fiber: how it can be affected by drying temperature. *Foods* **10**, 1–13 (2021).
7. Bozkir, H. & Ergün, A. R. Effect of sonication and osmotic dehydration applications on the hot air drying kinetics and quality of persimmon. *LWT* **131**, 109704 (2020).
8. Lin, Z. et al. Steam blanching and ethanol pretreatment enhance drying rates and improve the quality attributes of apple slices via microstructure modification. *J. Food Process. Preserv.* **46**, 1–14 (2022).
9. Ando, Y. et al. Improvements of drying rate and structural quality of microwave-vacuum dried carrot by freeze-thaw pretreatment. *LWT* **100**, 294–299 (2019).
10. Loureiro, A. da C. et al. Cold plasma technique as a pretreatment for drying fruits: evaluation of the excitation frequency on drying process and bioactive compounds. *Food Res. Int.* **147**, 110462 (2021).
11. Ricce, C., Rojas, M. L., Miano, A. C., Siche, R. & Augusto, P. E. D. Ultrasound pre-treatment enhances the carrot drying and rehydration. *Food Res. Int.* **89**, 701–708 (2016).
12. Feng, M. et al. Individual and synergistic effect of multi-frequency ultrasound and electro-infrared pretreatments on polyphenol accumulation and drying characteristics of edible roses. *Food Res. Int.* **163**, 112120 (2023).
13. Santos, N. C. et al. Effect of pulse electric field (PEF) intensity combined with drying temperature on mass transfer, functional properties, and in vitro digestibility of dehydrated mango peels. *J. Food Meas. Charact.* **17**, 5219–5233 (2023).
14. Wang, M. et al. Freeze-thaw pretreatment improves the vacuum freeze-drying efficiency and storage stability of goji berry (*Lycium barbarum*, L.). *LWT Food Sci. Technol.* **189**, 115439 (2023).
15. Vallespir, F., Rodríguez, Ó., Eim, V. S., Rosselló, C. & Simal, S. Effects of freezing treatments before convective drying on quality parameters: vegetables with different microstructures. *J. Food Eng.* **249**, 15–24 (2019).
16. Llavata, B., García-Pérez, J. V., Simal, S. & Cárcel, J. A. Innovative pre-treatments to enhance food drying: a current review. *Curr. Opin. Food Sci.* **35**, 20–26 (2020).
17. Shorstkii, I. et al. Correlation of the cell disintegration index with Luikov's heat and mass transfer parameters for drying of pulsed electric field (PEF) pretreated plant materials. *J. Food Eng.* **316**, 110822 (2022).
18. Malakar, S. et al. Application of novel pretreatment technologies for intensification of drying performance and quality attributes of food commodities: a review. *Food Sci. Biotechnol.* **32**, 1303–1335 (2023).
19. Kim, S. Y. et al. A pulsed electric field accelerates the mass transfer during the convective drying of carrots: drying and rehydration kinetics, texture and carotenoid content. *Foods* **12**, 589 (2023).
20. Polachini, T. C. et al. Hot-air ultrasound-assisted drying of green wheat and barley malts to enhance process kinetics, amylase activity and their application in bread formulation. *Food Bioprod. Process.* **142**, 17–28 (2023).
21. Szadzińska, J., Mierzwa, D. & Musielak, G. Ultrasound-assisted convective drying of white mushrooms (*Agaricus bisporus*). *Chem. Eng. Process. Process Intensif.* **172**, 108803 (2022).
22. García-Pérez, J. V. et al. Ultrasonic drying for food preservation. *Power Ultrasonics* 743–771 <https://doi.org/10.1016/B978-0-12-820254-8.00027-0> (Elsevier, 2023).
23. Ozuna, C., Álvarez-Arenas, T. G., Riera, E., Cárcel, J. A. & Garcia-Perez, J. V. Influence of material structure on air-borne ultrasonic application in drying. *Ultrason. Sonochem.* **21**, 1235–1243 (2014).
24. Zhu, R. et al. Dehydration of apple slices by sequential drying pretreatments and airborne ultrasound-assisted air drying: Study on mass transfer, profiles of phenolics and organic acids and PPO activity. *Innov. Food Sci. Emerg. Technol.* **75**, 102871 (2022).
25. Corrêa, J. L. G., Rasia, M. C., Mulet, A. & Cárcel, J. A. Influence of ultrasound application on both the osmotic pretreatment and subsequent convective drying of pineapple (*Ananas comosus*). *Innov. Food Sci. Emerg. Technol.* **41**, 284–291 (2017).
26. Rojas, M. L., Augusto, P. E. D. & Cárcel, J. A. Combining ethanol pretreatment and ultrasound-assisted drying to enhance apple chips by fortification with black carrot anthocyanin. *J. Sci. Food Agric.* **101**, 2078–2089 (2021).
27. Liu, Y. Y., Wang, Y., Lv, W. Q., Li, D. & Wang, L. J. Freeze-thaw and ultrasound pretreatment before microwave combined drying affects drying kinetics, cell structure and quality parameters of *Platycodon grandiflorum*. *Ind. Crops Prod.* **164**, 113391 (2021).
28. Xu, X. et al. Ultrasound freeze-thawing style pretreatment to improve the efficiency of the vacuum freeze-drying of okra (*Abelmoschus esculentus* (L.) Moench) and the quality characteristics of the dried product. *Ultrason. Sonochem.* **70**, 105300 (2021).
29. Mello, R. E., Fontana, A., Mulet, A., Corrêa, J. L. G. & Cárcel, J. A. PEF as pretreatment to ultrasound-assisted convective drying: Influence on quality parameters of orange peel. *Innov. Food Sci. Emerg. Technol.* **72**, 102753 (2021).
30. Llavata, B., Collazos-Escobar, G. A., Garcia-Perez, J. V. & Carcel, J. A. PEF pre-treatment and ultrasound-assisted drying at different temperatures as a stabilizing method for the up-cycling of kiwifruit: effect on drying kinetics and final quality. *Innov. Food Sci. Emerg. Technol.* **92**, 103591 (2024).
31. Zhang, T. et al. Dynamic changes of potato characteristics during traditional freeze-thaw dehydration processing. *Food Chem.* **389**, 133069 (2022).
32. Santos, N. C. et al. Impact of pretreatments with ethanol and freezing on drying slice papaya: drying performance and kinetic of ultrasound-

- assisted extraction of phenolics compounds. *J. Sci. Food Agric.* **103**, 125–134 (2023).
33. Guo, X. et al. An evaluation of different pretreatment methods of hot-air drying of garlic: drying characteristics, energy consumption and quality properties. *LWT* **180**, 114685 (2023).
 34. Chen, F., Zhang, M., Devahastin, S. & Yu, D. Comparative evaluation of the properties of deep-frozen blueberries dried by vacuum infrared freeze drying with the use of CO₂ laser perforation, ultrasound, and freezing–thawing as pretreatments. *Food Bioprocess Technol.* **14**, 1805–1816 (2021).
 35. Liu, C., Pirozzi, A., Ferrari, G., Vorobiev, E. & Grimi, N. Impact of pulsed electric fields on vacuum drying kinetics and physicochemical properties of carrot. *Food Res. Int.* **137**, 109658 (2020).
 36. Ostermeier, R., Giersemehl, P., Siemer, C., Töpfl, S. & Jäger, H. Influence of pulsed electric field (PEF) pre-treatment on the convective drying kinetics of onions. *J. Food Eng.* **237**, 110–117 (2018).
 37. Arevalo, P., Ngadi, M. O., Bazhal, M. I. & Raghavan, G. S. V. Impact of pulsed electric fields on the dehydration and physical properties of apple and potato slices. *Dry. Technol.* **22**, 1233–1246 (2004).
 38. Alam, M. R., Lyng, J. G., Frontuto, D., Marra, F. & Cinquanta, L. Effect of pulsed electric field pretreatment on drying kinetics, color, and texture of parsnip and carrot. *J. Food Sci.* **83**, 2159–2166 (2018).
 39. Pérez-Won, M. et al. Pulsed electric fields as pretreatment for different drying methods in Chilean abalone (*Concholepas concholepas*) mollusk: effects on product physical properties and drying methods sustainability. *Food Bioprocess. Technol.* **16**, 2772–2788 (2023).
 40. Wiktor, A. et al. Sustainability and bioactive compound preservation in microwave and pulsed electric fields technology assisted drying. *Innov. Food Sci. Emerg. Technol.* **67**, 102597 (2021).
 41. Garcia-Pérez, J. V., Cárcel, J. A., Riera, E. & Mulet, A. Influence of the applied acoustic energy on the drying of carrots and lemon peel. *Dry. Technol.* **27**, 281–287 (2009).
 42. Mello, R. E., Fontana, A., Mulet, A., Correa, J. L. G. & Cárcel, J. A. Ultrasound-assisted drying of orange peel in atmospheric freeze-dryer and convective dryer operated at moderate temperature. *Dry. Technol.* **38**, 259–267 (2020).
 43. Llavata, B., Femenia, A., Clemente, G. & Cárcel, J. A. Combined effect of airborne ultrasound and temperature on the drying kinetics and quality properties of Kiwifruit (*Actinidia Deliciosa*). *Food Bioprocess. Technol.* **17**, 440–451 (2023).
 44. Vallespir, F., Rodríguez, Ó., Eim, V. S., Rosselló, C. & Simal, S. Freezing pre-treatments on the intensification of the drying process of vegetables with different structures. *J. Food Eng.* **239**, 83–91 (2018).
 45. Bassey, E. J., Sun, D. W., Esua, O. J. & Cheng, J. H. Effects of freeze-thaw pretreatments on the drying characteristics, physicochemical and phytochemical composition of red dragon fruit during mid- and near-infrared drying. *Dry. Technol.* **41**, 561–576 (2023).
 46. Rojas, M. L. et al. Convective drying of cambuci, a native fruit from the Brazilian Atlantic Forest: effect of pretreatments with ethanol and freezing. *J. Food Process Eng.* **44**, 1–11 (2021).
 47. Yamakage, K. et al. Impact of pre-treatment with pulsed electric field on drying rate and changes in spinach quality during hot air drying. *Innov. Food Sci. Emerg. Technol.* **68**, 102615 (2021).
 48. Sánchez-Torres, E. A. et al. Airborne ultrasonic application on hot air-drying of pork liver. Intensification of moisture transport and impact on protein solubility. *Ultrason. Sonochem.* **86**, 106011 (2022).
 49. Wiktor, A. et al. The effect of pulsed electric field on drying kinetics, color, and microstructure of carrot. *Dry. Technol.* **34**, 1286–1296 (2016).
 50. Zongo, P. A., Khalloufi, S., Mikhaylin, S. & Ratti, C. Pulsed electric field and freeze-thawing pretreatments for sugar uptake modulation during osmotic dehydration of mango. *Foods* **11**, 2551 (2022).
 51. Noshad, M. & Ghasemi, P. Influence of freezing pretreatments on kinetics of convective air-drying and quality of grapes. *Food Biosci.* **38**, 100763 (2020).
 52. Faridnia, F., Burritt, D. J., Bremer, P. J. & Oey, I. Innovative approach to determine the effect of pulsed electric fields on the microstructure of whole potato tubers: Use of cell viability, microscopic images and ionic leakage measurements. *Food Res. Int.* **77**, 556–564 (2015).
 53. Puig, A., Perez-Munuera, I., Carcel, J. A., Hernando, I. & Garcia-Perez, J. V. Moisture loss kinetics and microstructural changes in eggplant (*Solanum melongena* L.) during conventional and ultrasonically assisted convective drying. *Food Bioprod. Process.* **90**, 624–632 (2012).
 54. Chao, E., Li, J. & Fan, L. Enhancing drying efficiency and quality of seed-used pumpkin using ultrasound, freeze-thawing and blanching pretreatments. *Food Chem.* **384**, 132496 (2022).
 55. Deng, L. Z. et al. Hot air impingement drying kinetics and quality attributes of orange peel. *J. Food Process. Preserv.* **44**, 1–11 (2020).
 56. Phuon, V., Ramos, I. N., Brandão, T. R. S. & Silva, C. L. M. Assessment of the impact of drying processes on orange peel quality characteristics. *J. Food Process Eng.* **45**, 13794 (2022).
 57. Garcia-Perez, J. V., Ortuño, C., Puig, A., Carcel, J. A. & Perez-Munuera, I. Enhancement of water transport and microstructural changes induced by high-intensity ultrasound application on orange peel drying. *Food Bioprocess. Technol.* **5**, 2256–2265 (2012).
 58. Kammoun Bejar, A., Boudhrioua Mihoubi, N. & Kechaou, N. Moisture sorption isotherms—experimental and mathematical investigations of orange (*Citrus sinensis*) peel and leaves. *Food Chem.* **132**, 1728–1735 (2012).

Acknowledgements

This work was supported by the PID2019-106148RRC42 grant funded by MCIN/AEI/ 10.13039/501100011033; PID2022-136889OB-C22 grant funded by MCIN/AEI/10.13039/501100011033/ERDF, a way of making Europe, and the Ph.D. grant of Beatriz Llavata from the Universitat Politècnica de València (PAID-01-19). We are also grateful for the economic support of the Coordenação de Aperfeiçoamento de Pessoal de Nível Superior – Brasil (Capes)—Finance Code 001, Conselho Nacional de Desenvolvimento Científico e Tecnológico (CNPq) and Fundação de Amparo a Pesquisa de Minas Gerais (FAPEMIG).

Author contributions

Conceptualization, J.A. Cárcel; methodology, B. Llavata, R.E. Mello, A. Quiles, J.A. Cárcel; software, B. Llavata, R.E. Mello, J.A. Carcel; validation, B. Llavata, R.E. Mello, A. Quiles and J.A. Carcel; formal analysis, B. Llavata, A. Quiles, J.L.G. Correa, J.A. Carcel; investigation, B. Llavata and R.E. Mello; resources, B. Llavata, J.A. Cárcel; data curation, B. Llavata and J.A. Carcel; writing—original draft preparation, B. Llavata, R.E. Mello; writing—review and editing, B. Llavata, A. Quiles, J.L.G. Correa and J.A. Carcel, ; supervision, J.L.G. Correa, J.A. Cárcel; project administration, B. Llavata; funding acquisition, J.A. Cárcel. All authors have read and agreed to the published version of the manuscript.

Competing interests

The authors declare no competing interests.

Additional information

Correspondence and requests for materials should be addressed to Juan A. Cárcel.

Reprints and permissions information is available at <http://www.nature.com/reprints>

Publisher's note Springer Nature remains neutral with regard to jurisdictional claims in published maps and institutional affiliations.

Open Access This article is licensed under a Creative Commons Attribution-NonCommercial-NoDerivatives 4.0 International License, which permits any non-commercial use, sharing, distribution and reproduction in any medium or format, as long as you give appropriate credit to the original author(s) and the source, provide a link to the Creative Commons licence, and indicate if you modified the licensed material. You do not have permission under this licence to share adapted material derived from this article or parts of it. The images or other third party material in this article are included in the article's Creative Commons licence, unless indicated otherwise in a credit line to the material. If material is not included in the article's Creative Commons licence and your intended use is not permitted by statutory regulation or exceeds the permitted use, you will need to obtain permission directly from the copyright holder. To view a copy of this licence, visit <http://creativecommons.org/licenses/by-nc-nd/4.0/>.

© The Author(s) 2024